

Frascati, January 15, 2007

Note: LC-7

**ELECTROMAGNETIC-THERMAL ANALYSIS OF AN X-BAND LINAC
STRUCTURE BY FINITE ELEMENT SIMULATIONS***L. Quintieri, F. Tazzioli***Introduction**

The design of RF structures for particle accelerators requires an accurate estimation of the sensitivity to the mechanical deformations induced by the surface power loss on the metallic walls. The prediction of these effects is important for conceiving a tuning strategy that assures the structure correctly operates when integrated into the accelerator complex. The work presented in this report has to be located in this frame. In fact a new experimental technique has been proposed to predict change in cavity frequency due to mechanical deformations for various thermal loads, using a thermal radiator. A multi-physics finite-element code (ANSYS) has allowed comparing, for the same heat power generated, the thermal distribution inside the structure due respectively to radiation heat and electromagnetic power loss produced in the π -mode. The comparison shows that the radiation heating by an internal heater could be effectively used for testing the frequency change under thermal load, encouraging to develop and qualify a methodology that can be easily and relatively cheaply implemented in laboratory.

1. Work description

The main objective of this work is to demonstrate that it is possible to use a thermal radiator for testing the temperature distribution and the consequent stress and strain field inside the cavity to estimate how much the induced mechanical deformation can affect the frequency of the cavity. The preliminary comparison shows that, even if the temperature profile in case of radiation heating is flatter than that induced by the rf-surface power loss, such alternative system could be effectively used and with some improvements could fully reproduce the RF-real case.

In this paper we report:

- The comparison between measurements of the temperature in a RF cavity heated by a thermal radiator for several input powers, as documented in [1], and numerical simulations of the experimental cases (using ANSYS finite element code). The good agreement between the measured and the calculated values of temperature has made us confident in having a validated 2D model for the radiation heat-exchange calculations, so that we can effectively use it to do previsions about the mechanical strain and stress field, inside the cavity.
- The comparison between the estimated temperature distribution inside the cavity in the case of radiation heating and in the case of induced electromagnetic power loss, for the same input power. In fact we want to check if the temperature profile in the case of external radiation heating can approximate the temperature profile due to the electromagnetic surface power loss and consequently understand if the experimental data from the radiation heating case could be effectively used to foresee the actual mechanical strain in a cavity under electromagnetic load.

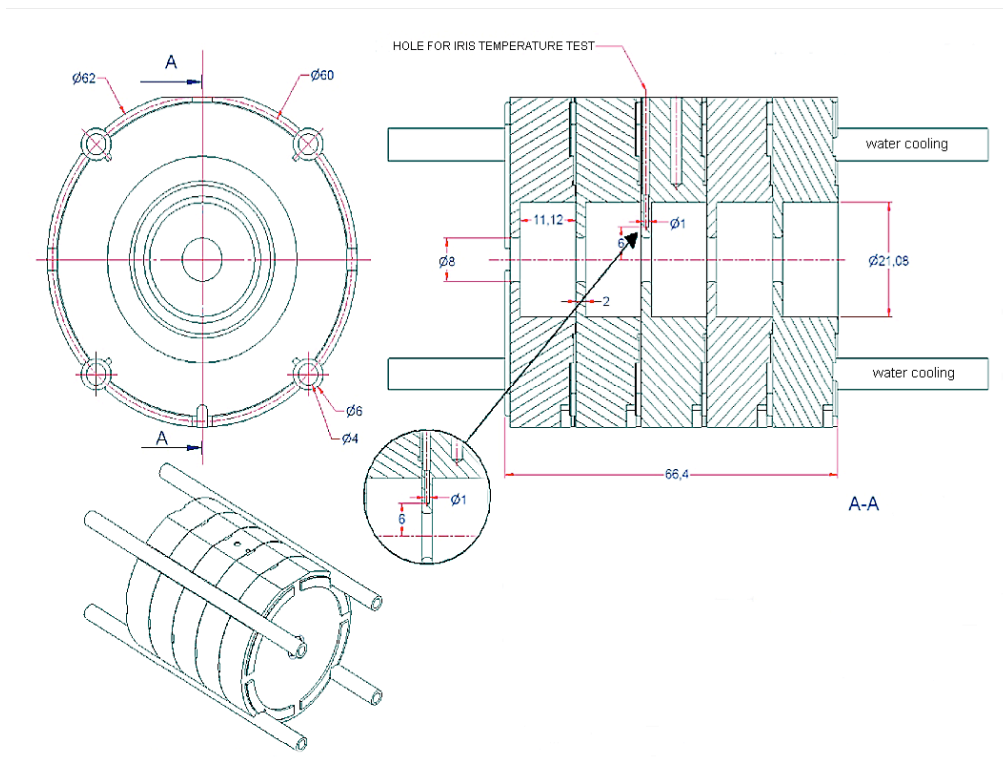


Figure 1: Experimental set-up.

The RF-cavity that has been used for our tests is a high-frequency accelerating structure designed to be operative for the SPARC project (Sorgente Auto-amplificata di Radiazione Coerente) [2].

Finite element analysis has been carried out using the Ansys software [3]. ANSYS is a multi-physics environment that includes a High Frequency solver module and we use it to perform coupled analysis: Radio/Frequency-Thermal/Mechanical. The High Frequency module has for the moment the limitation that only 3D elements can be used, so 3D simulations have to be performed also for virtually 2D problems (e.g. axis-symmetric structures where the modes of interest are also symmetric around geometric axis).

The finite element analysis has been carried out in two steps:

1. A 2D model has been used for evaluating the radiation heat exchange between the thermal radiator and the cavity. In addition the thermal stress and strain field induced by the temperature gradients in the structure, in steady-state condition, have been estimated. The results obtained from these calculations have been compared with the experimental values, giving a satisfactory agreement (an accordance within 17% in the worst case), taking also into account the uncertainty with which we know some material properties especially about the surface emissivity.
2. A 3D model has been created for developing a coupled high-frequency electromagnetic and thermal analysis. The temperature profile has been calculated, supposing to have the cavity operating in continuous regime at the designed π -mode frequency (11.4 GHz). The magnetic field intensity has been chosen in order to perform a coherent comparison with the power heating used in the laboratory tests.

2. Thermal Radiation Heat Exchange Calculation: the 2D ANSYS Model

The experimental set-up is shown in figure 1, where the dimensions of the cavity and the thermocouple hole are displayed, while in figure 2, the finite element model used for the numerical simulation is reported.

The FE Model: The two-dimensional model has been built, taking advantage of the symmetry of geometry, loads and boundary condition. A plane axisymmetric element (plane 55), with a 2-D thermal conduction capability, has been used for meshing the geometric domain. The thermal radiating bar, the cavity and the 2 small stainless-steel end-caps have been reproduced and meshed with uniform mesh size, small enough to accurately reproduce high localized thermal and strain gradients (0.5 mm is the maximum element size for a total of 6877 elements).

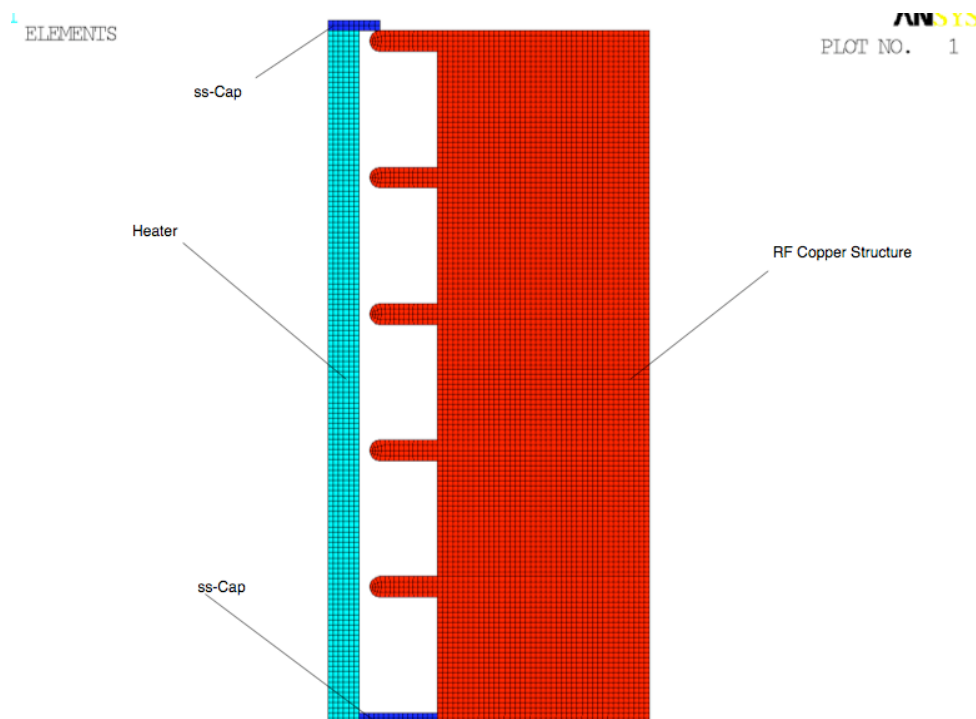


Figure 2: 2D Finite Element Model: the red structure is the copper cavity, the blue ones are the ss caps and the green one is the heater.

The Physic Domain: The internal surface of these elements delimits the physic enclosure for the radiation heat exchange. The enclosure in a radiation problem is a set of surfaces radiating to each other. ANSYS uses the definition of an enclosure to calculate the view factors¹, amongst surfaces belonging to an enclosure. Each radiating surface has an emissivity and a direction of radiation assigned to it. The emissivity is a surface radiative property defined as the ratio of the radiation emitted by the surface to the radiation emitted by a black body at the same temperature. ANSYS restricts radiation exchange between surfaces to gray-diffuse surfaces. The word grey

¹ The fraction of radiation leaving surface i which is intercepted by surface j.

signifies that emissivity and absorptivity of the surface do not depend on wavelength (either can depend on temperature). The word diffuse means that emissivity and absorptivity do not depend on direction. For a gray diffuse surface, emissivity = absorptivity; emissivity + reflectivity = 1 (black body surface has a unit emissivity). The Emissivity for a surface can be a function of temperature and depends on the manufactured and oxidation state of the surface. In table 1 the value of copper emissivity for several surface status are reported. For the radiator an emissivity equal to 0.9 has been assumed, instead an inner surface emissivity of 0.11 has been considered for the stainless steel (polished-machine rolled ss). In our experiment the heating has been realized in air, so that the internal surface of the copper resulted oxidized and consequently, in order to reproduce thermal boundary conditions as much close as possible to the reality, a value of 0.7 (see table 1) for the copper emissivity has been assumed for our calculations.

The Materials: The internal heater is a cylindrical bar of 6 mm diameter, made of a nichel-chrome alloy, whose thermal properties used in the calculation are reported in table 2, together with the properties of oxygen-free copper of which the cavity is made. This heater is able to generate a power up to 400 W and is mounted on the axis of the structure.

Table 1: Copper Emissivity

Surface State	Emissivity
commercial burnished	0.07
electrolytic polished	0.02
polished	0.031
polished annealed	0.008
oxidized	0.65
heavly oxidized	0.78
oxidized to black	0.88

Table 2: Material Properties (in the temperature range 293-320 K)

Thermal properties	Ni-Cr-alloy	OF Copper
Density [kg/m ³]	8470.0	8960.0
Thermal Conductivity [W/m K]	11.4	388.
Heat Capacity [J/kgK]	435.	383.
Thermal linear expansion	13.0E-6	16.4E-6

The Thermal Load: The aim of the calculation is to determine the temperature profile inside the cavity, due to the radiation heat exchange with the thermal radiator. Consequently the induced mechanical deformations have been estimated, by means of a “sequentially coupled physics” approach. The thermal load has been applied in the elements of the radiator as an internal heat power generation (using the ‘hgen’ command in ANSYS). Input power values from 60 to 250 W have been used in the developed calculations. An initial uniform temperature has been specified to be about 293 K for the cavity and the radiator.

The Boundary Conditions: The boundary condition has been imposed fixing the temperature on the external cavity surface, according to the measured steady-state values, for each input power applied. The convection heat exchange, by which the cavity is actually cooled, can be correctly introduced only with a 3D model, taking into account the not uniform heat-exchange on the external cavity surface. In fact the cavity is cooled by 4 copper tubes of 4 mm inner diameter (1mm wall tube thick), each placed 90 deg apart from each other. Anyway in order to predict the maximum achievable ΔT in the cavity also in case of heat flow rates higher than that experimentally used (heating power greater than 200 W), a convection heat exchange boundary condition has been introduced on the external nodes of the cavity, in such a way to balance exactly the input power. In fact, because we want to estimate the stationary distribution of temperature, the net heat flow rate through the cavity has to be zero, otherwise the temperature profile would change with time. We supposed that all the nodes of the external cavity boundary exchange by convection with a water flow corresponding to the real one (14 g/sec), while the average convection coefficient has been estimated using the experimental values derived from measurements at lower power, (60-100-150W) according to this equation:

$$h = \frac{\dot{Q}}{S \cdot \Delta T_w} \quad (1)$$

where Q-dot is the heating power generated in the radiator, S is not the effective heat-exchange surface but the total external one and ΔT_w is the difference between the cavity surface temperature and the water bulk temperature (this one being estimated by averaging the inlet and outlet water temperature in the tubes). The h estimated according to the equation 1 has been used to calculate the temperature difference for the two highest power values in figure 3 (200-250 W).

The Numeric Solver: Because the radiation heat flow varies with the fourth power of the body's absolute temperature, radiation analyses are highly nonlinear. The numerical method used to simulate the radiation heat exchange is the Radiosity one that accounts for the heat exchange between radiating bodies by solving for the outgoing radiative flux for each surface, when the temperatures for all surfaces are known. The surface fluxes provide boundary conditions to the finite element model for the conduction process analysis.

2.1 Calculation Results

The maximum temperature gradient in the cavity has been determined versus the input power in the radiator: the calculated values are shown in figure 3 and are compared with the measured ones in table 3.

Table 3: Comparison between results from ANSYS simulation and measured values

Input Heat Rate[W]	Measured T [K] ± 0.2	Calculated T [K]
60	1.	1.04
100	2.	1.72
150	4.	2.7

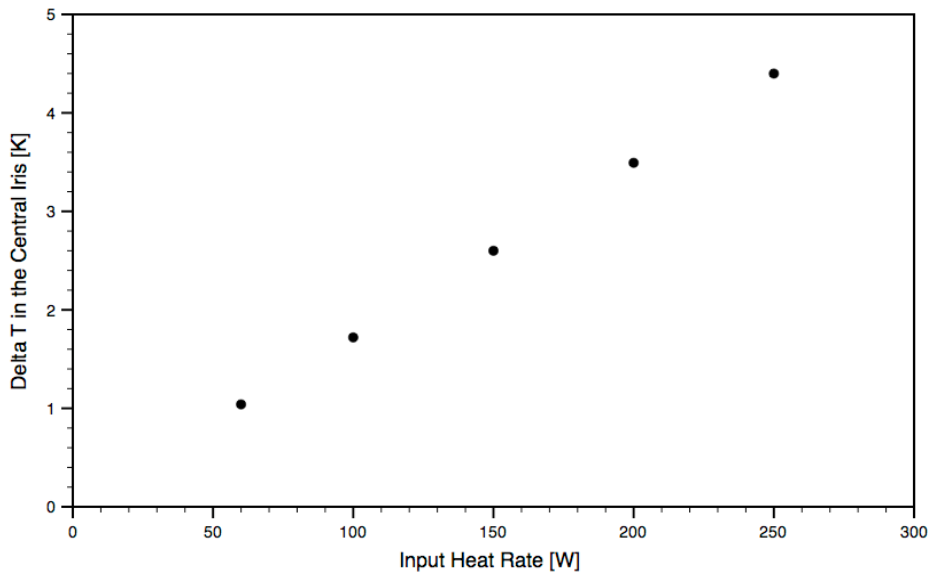


Figure 3: Calculated ΔT versus Input Power.

The reliability of the results depends strongly on the mesh of the model. Comparing the nodal solution with the element one, for every calculation, we found a difference less than 6% so that we can be sure to have used a sufficient refined mesh.

In figure 4 we report the temperature profile calculated inside the cavity for the case of 150 W, while in figure 5, the radial temperature profile in correspondence of the central iris (from the tip of the iris to the external cavity surface), where the thermocouple has been placed, is reported.

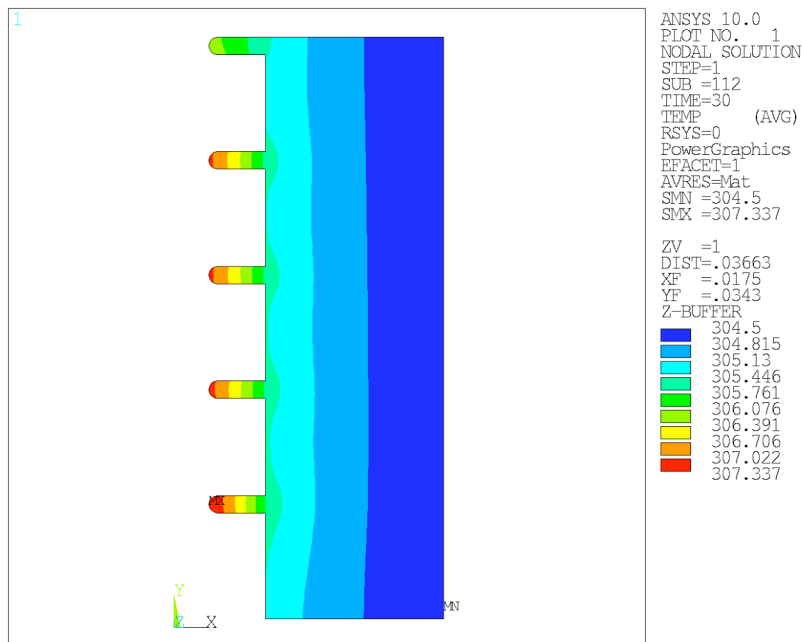


Figure 4: Temperature Field in the cavity for 150 W (radiation heating).

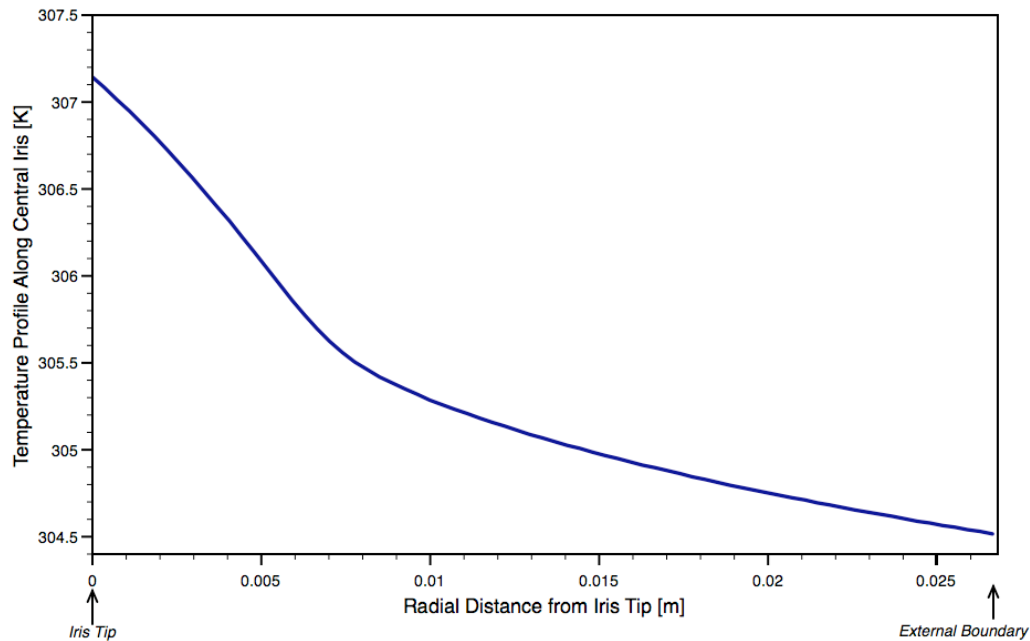


Figure 5: Radial Temperature Profile for 150 W radiation heating (from the tip of the central iris to the external cavity surface).

As a result of this analysis we can conclude that the calculated values reproduce the experimental results within a 25% of accuracy: the agreement between calculations and measurements is excellent for low heating power and less satisfactory for the higher ones. It is important to underline that in the 2D calculations the actual not uniform heat exchange by convection, on the external boundary surface, has been replaced by a uniform fixed temperature condition or by a uniform convective heat exchange on the external surface², that surely contributes to have a flatter temperature profile. Anyway, we have to consider that by increasing the input power, other mechanisms of heat exchange, related to the presence of air inside the cavity, could take place and, even though less important than radiation, could affect the temperature distribution inside the cavity. In order to estimate this possibility, we have simulated the air inside the cavity and we have taken into account the thermal conductivity through it. The air has been considered completely transparent respect to the radiation.

In figure 6 and 7 we report the results of the calculations in presence of air in the cavity. If we consider the conduction of air, taking also into account that the air thermal conductivity ranges from 26.3E-3 W/mK at 300 K to 76.3 E-3W/mK at 1200 K, we calculate an increase of about 22% of the temperature difference in case of 150 W (in this case $T_{\max} = 3.3$ K instead of 2.7 K).

² The convective heat exchange inside the water tube is going to be accomplished and included as next step in the 3D complete model.

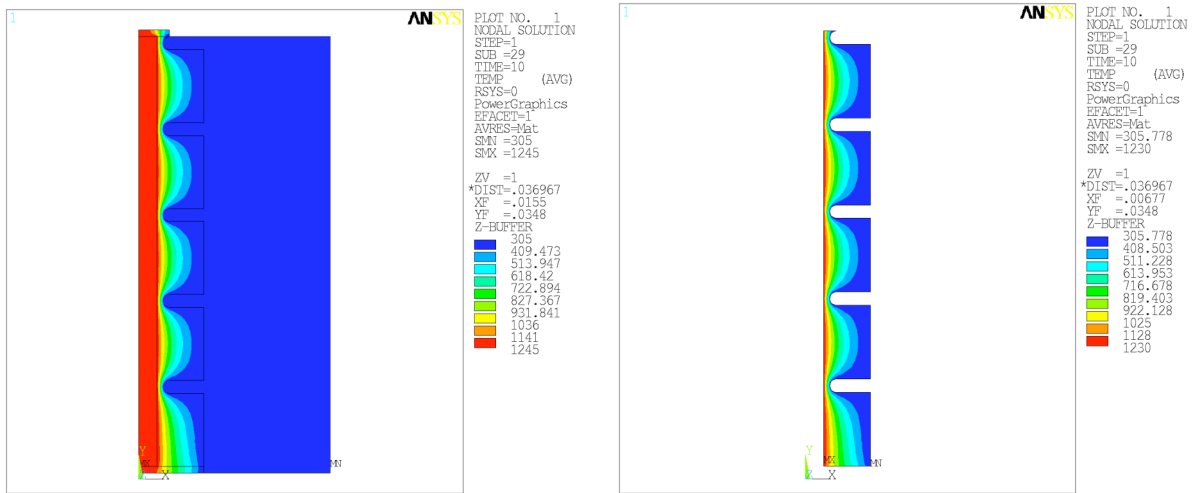


Figure 6: Temperature field inside the cavity with air in case of 150 W heat flow rate (on the right air only).

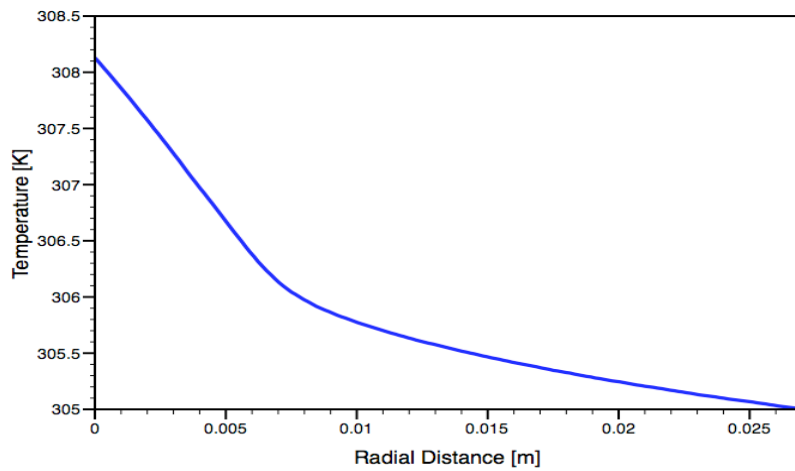
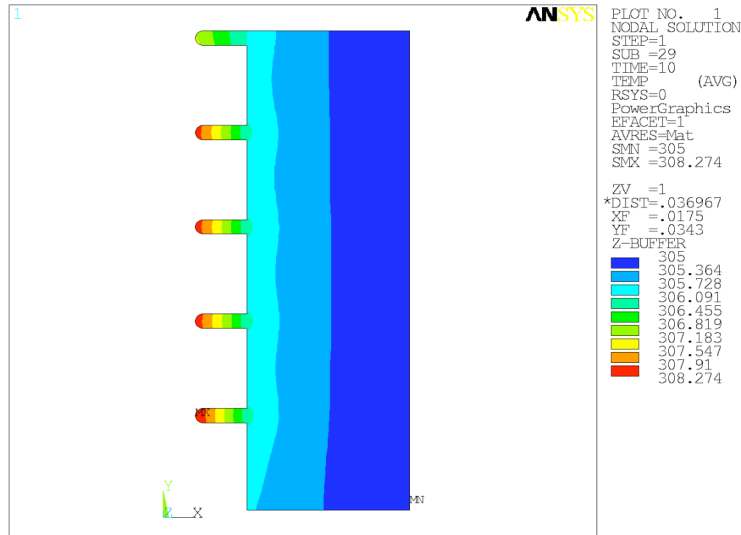


Figure 7: On the top, temperature field in the copper structure with air for 150 W radiating power. On the bottom, radial temperature profile on the inner iris.

In table 4 the results for the calculations with and without air are summarized, comparing them with the experimental values.

Table 4: Comparison between results from ANSYS simulations and measured values

Heating Power [W]	Measured T [K]	T [K] without air	T [K] with air
60	1.	1.04	1.3
100	2.	1.72	2.1
150	4.	2.7	3.3

Measurements made under vacuum could be useful to check these results and moreover it could be useful to measure the temperature in the other irises, to compare the experimental axial temperature profile in the cavity with that estimated by the finite element method.

In conclusion, in order to check in the most accurate way the effectiveness of this proposed method, we encourage a next campaign of measurements voted to produce a complete temperature map inside the cavity.

2.2 The Coupled Thermo-Structural Calculation

For evaluating the strain induced by the temperature gradient we refer to a model of the cavity without end caps (a completely symmetric structure with 6 irises) and having the mechanical constraints that the cavity should have when put into operation on the beam transfer line. The input power has been considered to be generated by means of an internal heater with uniform power density (to analyze the experimental case): as it will be shown later in this report, the axial temperature profile calculated in this case is flatter than that estimated for the electromagnetic power loss, while the radial one, is fully similar in the two cases. The axial temperature along the inner profile of the cavity is shown in figure 8, while the temperature on the internal diameter of the cylinder (at the iris bases) is shown in figure 9: the profile in both the cases shows a peak at the center of each iris, as expected, and is symmetric around the middle of the cavity, the inner irises being hotter than the external ones.

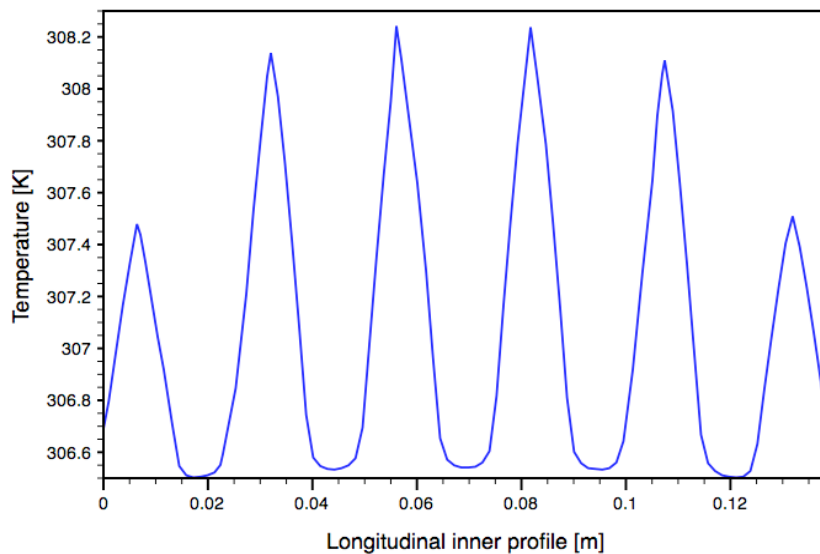


Figure 8: Axial Temperature Profile in the Cavity (along the inner surface of the cavity) in case of uniform heating power density.

The temperature field along the axis cavity is not uniform because the six irises are not exactly subjected to the same thermal loads: the inner ones are in fact warming little more than the external ones. This is due to the different view factors by which the external irises receive heating only from internal side. The maximum temperature on the two external irises is about 1.5 K (50% of T_{\max}) lower respect to the inner ones, where the maximum value of about 308 K is reached. This difference of temperature is reduced at about 2 tenth of degree on the bulk material (see figure 9): but if we refer to the maximum ΔT at a fixed radius (i.e. along the diameter corresponding to the iris bases), the external irises have a ΔT 40% less than the internal one.

ANSYS

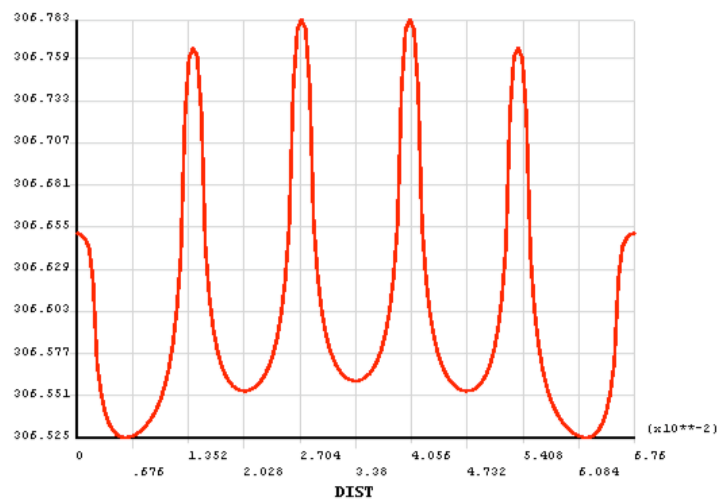


Figure 9: Axial Temperature Profile in the Cavity (along the inner diameter at the iris bases) in case of uniform heating power density.

As a result of the 3D RF-thermal calculations, discussed later in paragraph 3, the temperature profile in the cavity is characterized by isothermal curves more peaked in the center (see figure 28) respect to the case of heating by a uniform thermal radiator. For this reason, we have studied also the possibility to amplify the peaked axial profile, already existing in the case of radiation heating, using a not uniform thermal heater.

Figure 10 shows how the temperature profile does change when the heating power density in the radiator is generated by a symmetric linear distribution (see figure 11).

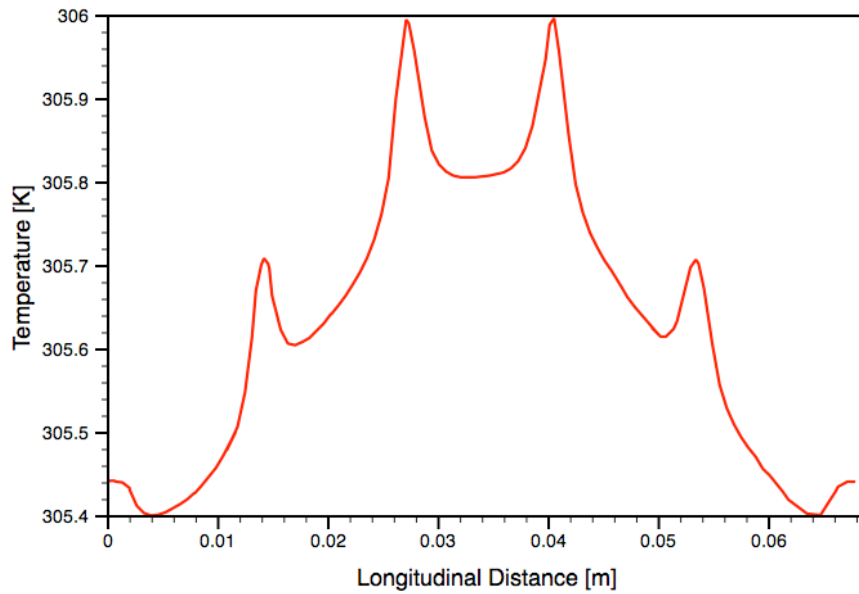


Figure 10: Axial Temperature profile in the cavity (along the inner diameter at the iris base) for a symmetric linear density power.

In this case we have imposed a density heating power, symmetric with respect to the middle of the heater, that in a coordinate frame with origin in this center can be expressed by the following equation:

$$W(x) = A - B \cdot x^2 \quad (2)$$

where A and B have to satisfy the following condition:

$$W(x = \pm L/2) = 0$$

where $\pm(L/2)$ are the coordinates of the heater extremities. In the case of linear power distribution we have increased by a factor 2.5 the maximum axial T along the inner diameter (from 0.2 K to 0.5 K). For a fixed value of the integral heating power, the shape of the power density distribution along the radiator could be the tunable parameter that we would adjust in order to reproduce in the cavity a thermal field as close as possible to that expected from radio-frequency excitation.

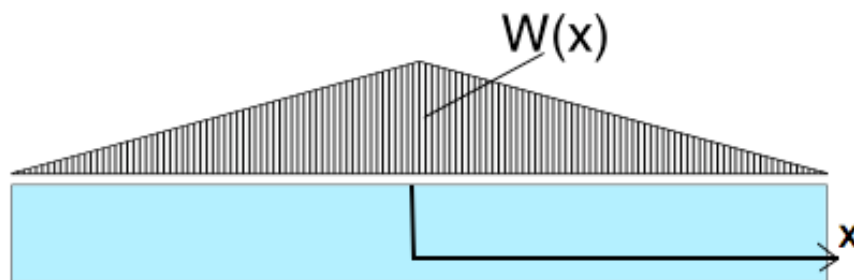



Figure 11: Symmetric linear distribution of the power heating inside the thermal radiator.

However it is important to underline that the RF calculations have been done for the cavity without electromagnetic field compensation³ that should reduce at few percent the difference between the field amplitude in each cell. In a compensated multi-cell cavity we expect to have a flatter thermal profile inside the cavity (the power loss being proportional to the square amplitude of the electromagnetic field), that means to approach closer the temperature distribution obtained by the radiation heating. Therefore, the next step of our work foresees to do the coupled calculations for the compensated cavity in order to compare the maximum longitudinal ΔT for the radiation case and the rf-power loss case⁴.

2.3 Strain Deformation Prediction

ANSYS allows the thermal elements (plane55 in our case) to be converted directly to structural elements (plane42) so to obtain the stress and displacement solution. The thermal distortion of the cavity is evaluated on the basis of the thermal expansion coefficient of the material (see table 2) and the nodal temperature data obtained from the thermal solution, applied as a load on the structural model (according the sequential scheme for coupled calculations). Furthermore the symmetry boundary condition and the support constraints are included in the model. The initial temperature with respect to which we estimate the thermal stress is the room temperature (i.e., $T=293$ K is the reference temperature at which the structure is supposed to be free of stress). Two calculations have been conducted in order to take into account different ideal boundary conditions: respectively cavity blocked at one end and free on the other one and cavity blocked at both ends. The detuning value lies in between these two numerical results. Forthcoming 3D detailed simulations taking into account the actual support frame are underway.

 **First case: one end blocked only.** The cavity is free to expand. In figure 12 the total displacement has been shown over the undeformed initial edges. The maximum displacement is obtained in correspondence of the free end of the cavity and is about $14 \mu\text{m}$. Each cell of the cavity expands by a longitudinal total displacement of about $3 \mu\text{m}$ between two consecutive irises, while the radial displacement is uniform on all the cells and is about $2 \mu\text{m}$. The Von-Mises equivalent total strain and stress is shown in figure 13 and 14, respectively: the maximum strain is located on the tips of the irises ($0.62\text{E-}4$) being the warmest regions in the cavity. The highest stresses in the cavity are caused by local thermal gradients between the hottest inner surface and the external cooled boundary and by the differential expansion of the warm regions with respect to the rest of the cavity. The maximum stress, on the tips of the irises, is equal to about 6.8 MPa (the yield stress in oxygen free copper being about 200 MPa).

³ This is realized reducing the inner radius of the outer cells of the resonant cavity.

⁴ The maximum radial difference on the central iris, as shown later, is quite the same in both cases.

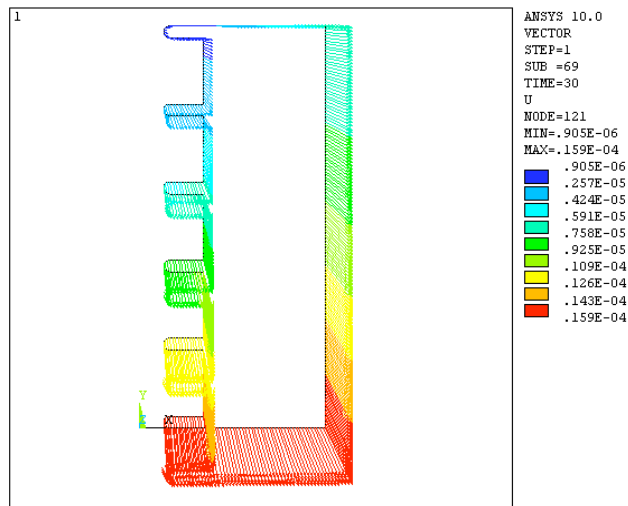


Figure 12: Total Displacement [m] in case of only one blocked end.

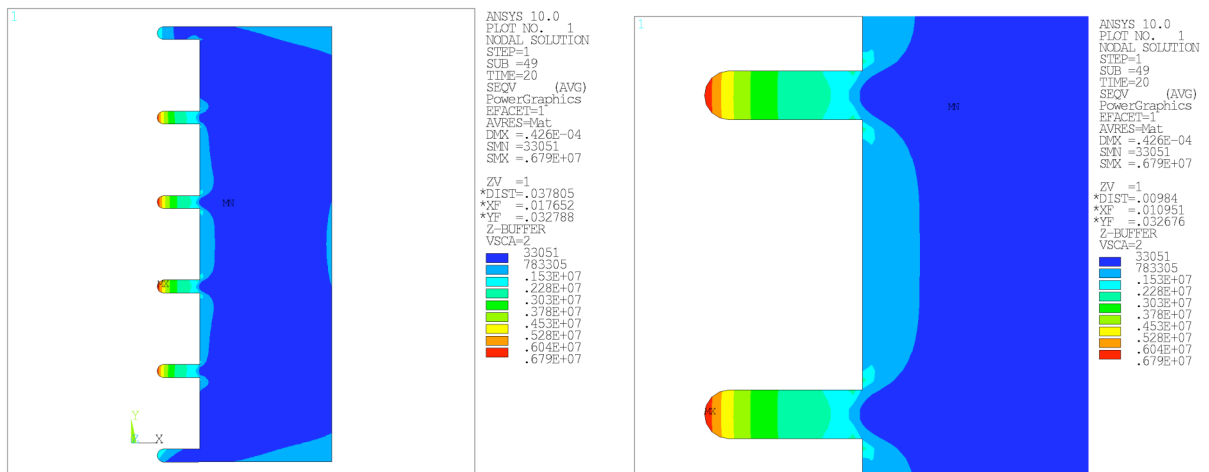


Figure 13: Von Mises Equivalent Stress [Pa] in case of only one blocked end.

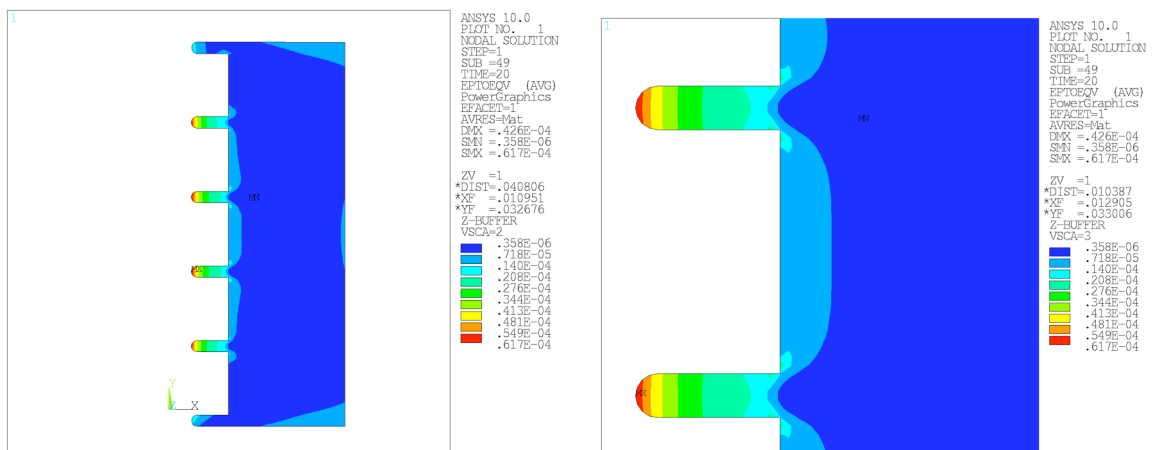


Figure 14: Von Mises Equivalent Strain in case of only one blocked end.

Second case: both ends constrained. The maximum stress is localized around the blocked irises: because of the discontinuity of section at the iris base, there are high values of stress (near the yield stress) and stress gradient, that could cause local plasticity (see figure 16). In figure 15 the final structural deformation has been shown: the maximum displacement happens on the external surface (about $9\mu\text{m}$), while the internal cells of the cavity have a differentiate behavior: the external ones are compressed with a maximum longitudinal contraction on of about $3\mu\text{m}$ and a radial expansion of about $2.5\mu\text{m}$ respect to the initial position. The central one is stretched in longitudinal direction of about $1\mu\text{m}$ and expands in radial direction of about $2\mu\text{m}$.

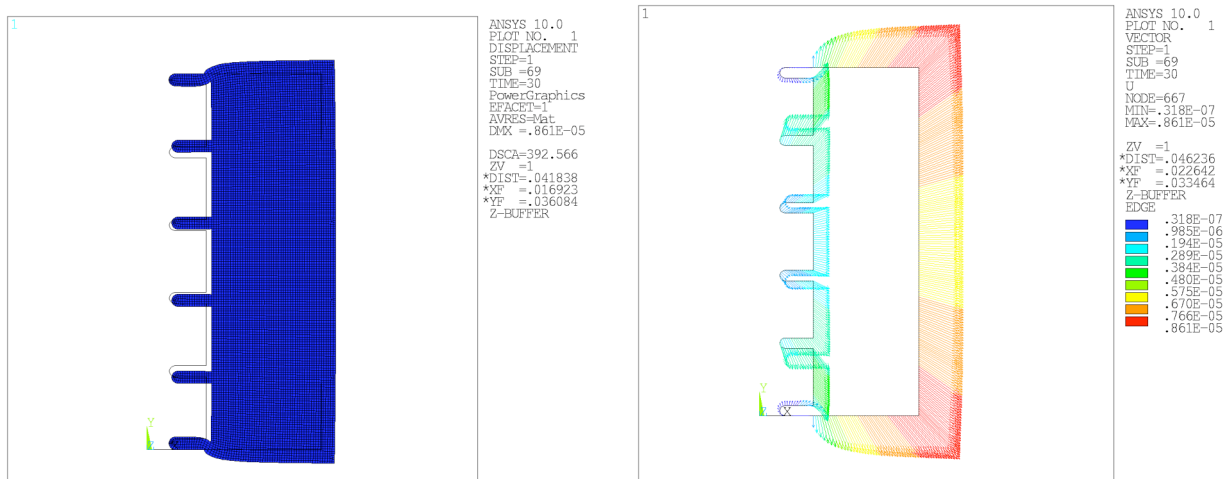


Figure 15: Total Displacements [m] in case of both ends blocked.

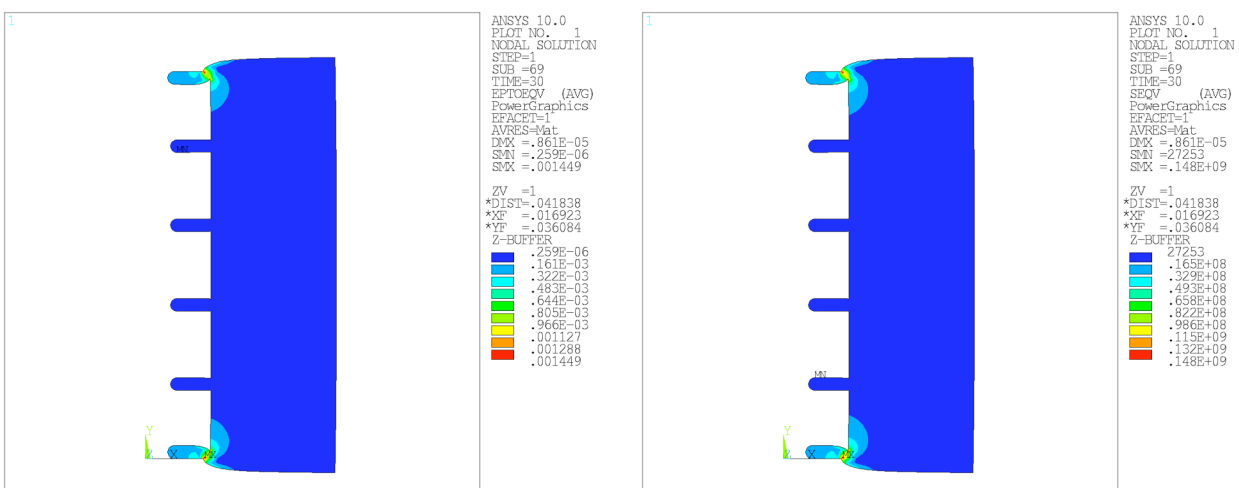


Figure 16: on the left, Equivalent Von-Mises Strain, and on the right, Equivalent Von Mises Stress[Pa], (both ends constrained).

The above cases allow to put limits on the maximum expected displacements both in radial and longitudinal direction: the maximum longitudinal elongation of the cell should be less than $9\mu\text{m}$ from the first case, while the maximum radial elongation (in the central cell) should not exceed $2.5\mu\text{m}$ (from the second case).

3 The 3-dimensional Coupled Analysis: Electromagnetic-Thermal

The commercial finite-element code ANSYS provides the ability to link electromagnetic to thermal and structural analyses. For version after 5.4, Ansys provides the high-frequency (HF) analysis module and associate elements. This module has been applied in order to evaluate the RF loss and the consequent temperature distribution in our cavity. A coupled field analysis by a unique code is more efficient respect to using different specialized software. In fact the exchange of information between electromagnetic field simulators and structural/thermal simulators can be difficult and can lead to errors. In case of multi-physics code like ANSYS this exchange of information between different modules is a built-in feature of the software, so that the model can be established by one single software and related data can be transferred more efficiently and easily in between elements due to same mesh employed.

3.1 The 3D model

The initial phase of the analysis consists of a high frequency electromagnetic calculation on the inner vacuum volume. The model is composed of a solid 3-dimensional volume representing the inner vacuum of the cavity plus two short cylindrical volumes on the extremities (representing the vacuum volume of the beam-line). In order to reduce the CPU time for calculation, the model has been constructed taking advantage of symmetry conditions. Only 45° of the whole structure has been meshed, using tetrahedral RF elements (HF119) with uniform fine mesh (for a total of 24575 elements only for the vacuum).

HF119 is a high-frequency tetrahedral element which models 3-D electromagnetic fields and waves governed by the full set of Maxwell's equation in linear media. HF119 applies to the full-harmonic and modal analysis but not to the transient analysis. Even if the electromagnetic results are fairly insensitive to mesh density, however the surface heat flux is highly dependent on the mesh size at the cavity wall-to-vacuum boundary. A satisfactory mesh has been generated by an iterative process with the goal to have a heat flux on external boundary not depending on the mesh size (the magnetic fields at the surface and thus the surface heat fluxes are accurately depicted while minimizing CPU time and memory usage). Figure 17 shows the meshed vacuum volume used to obtain the electromagnetic solution.

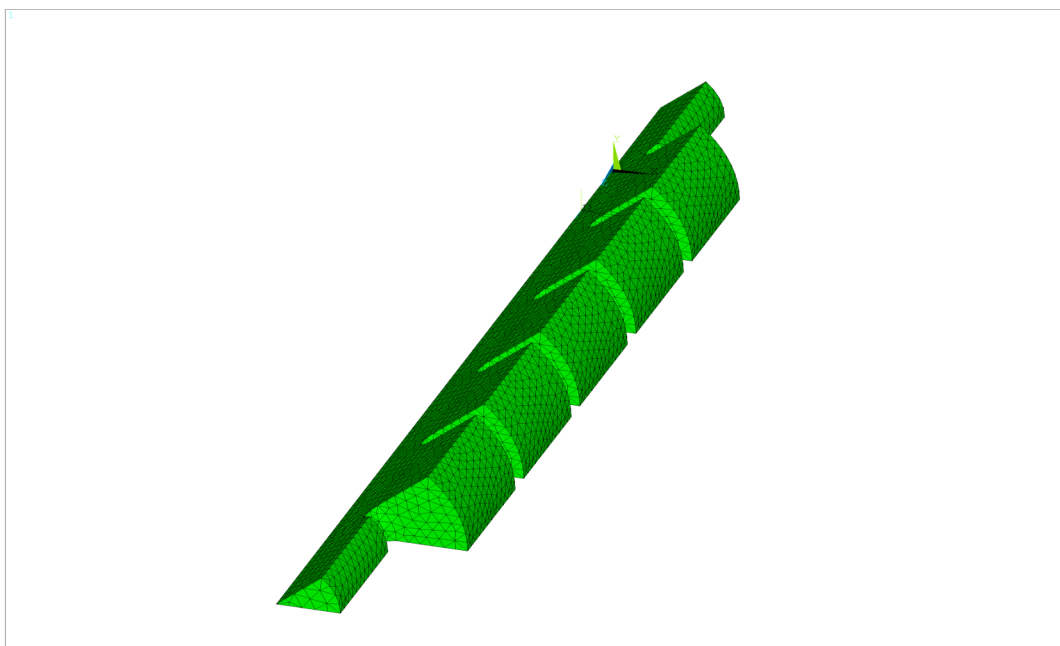


Figure 17: Element plot of the symmetric RF model.

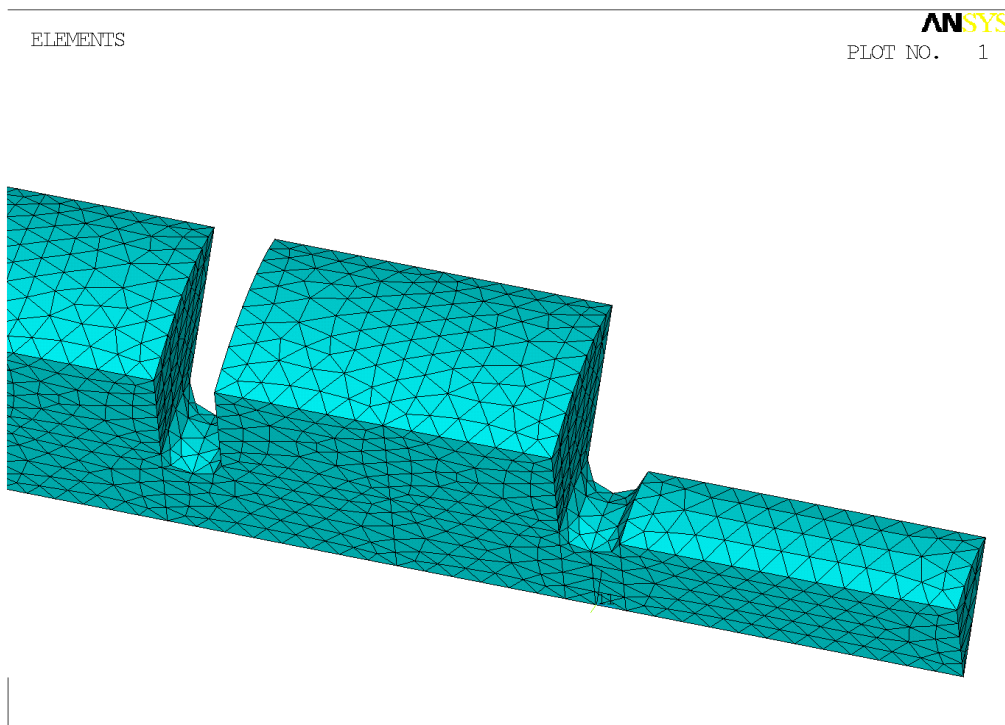


Figure 18: A zoom on a limited zone of the meshed vacuum volume.

Electric wall conditions (electric field normal to the wall-to-vacuum surface) are applied to the exterior surface of the whole vacuum volume, whereas the impedance boundary conditions (surface resistivity) are applied only on the cavity interior surface like surface load (sf command with keyword shld), as is shown in figure 19.

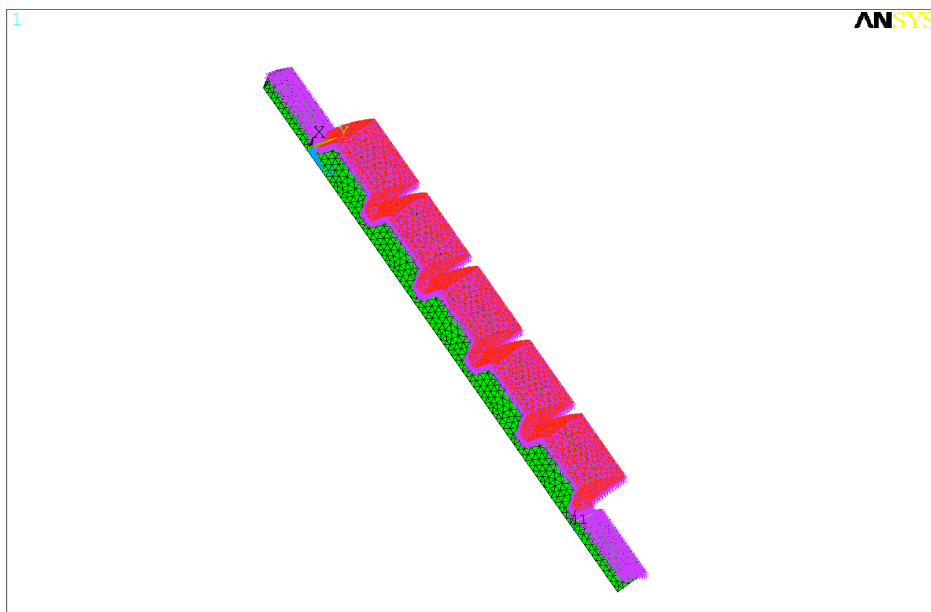


Figure 19: 3D Boundary conditions: tangential electric field vanishes on the vacuum-to-wall surface (the violet symbols) and surface resistivity applied on internal wall of the copper cavity (the red symbols).

No boundary conditions have to be applied to the model's symmetry planes since in ANSYS unconstrained surfaces are set by default to magnetic walls⁵. Note that the cavity ports have not yet been incorporated in the model.

3.2 High-Frequency Electromagnetic Calculation

3.2.1 Modal Analysis

The modal analysis allows to individuate the working frequency of the mode, for which we intend to develop the harmonic analysis. The natural modes of the cavity have been extracted between 10.5e+9 and 15.e+9 Hz using the Block Lanczos numerical solver⁶.

In this frequency range there are 5 resonances: the first 4 are shown in figure 20 and 21 (electric and magnetic field respectively), while the magnetic and electric field of the π -mode (11.4 GHz), in which we are interested, is reported in figure 22.

Table 5: Resonance Frequencies

Mode	Frequency [Hz] · 10 ⁹
1	11.178
2	11.228
3	11.297
4	11.368
5	11.422

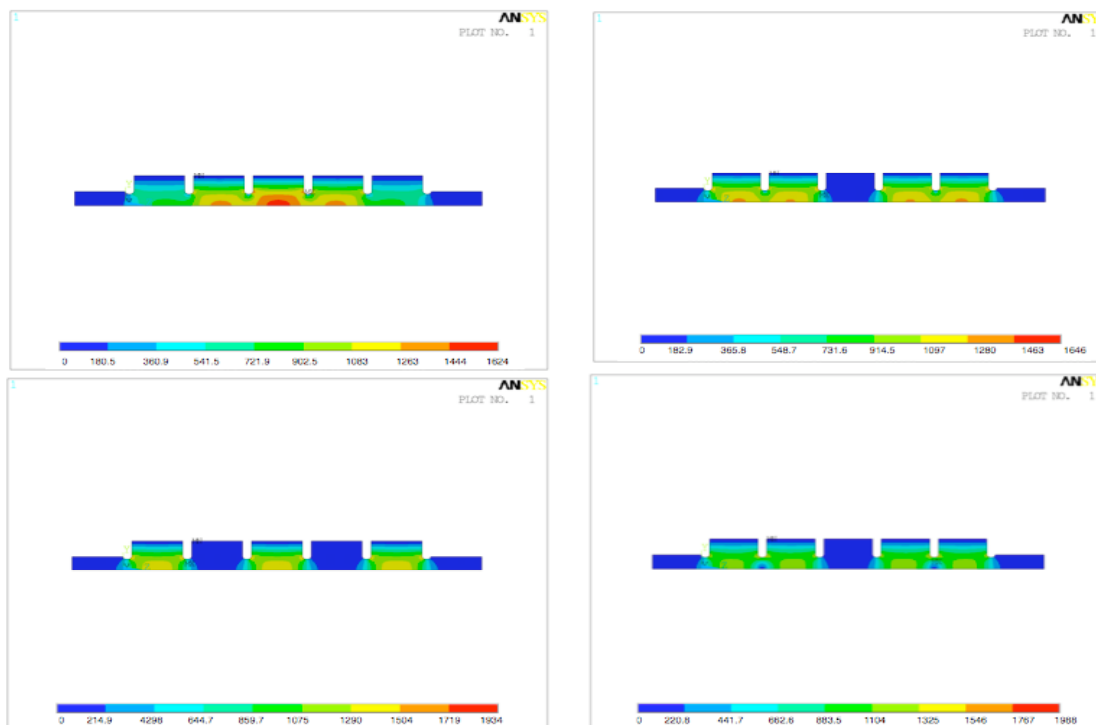


Figure 20: Electric Field (EFSUM[V/m]).

⁵ The magnetic wall is defined as a surface on which the tangential component of the vector magnetic field vanishes.

⁶ ANSYS calculates the element results in the form of normalized electric and magnetic field vectors and flux density vectors.

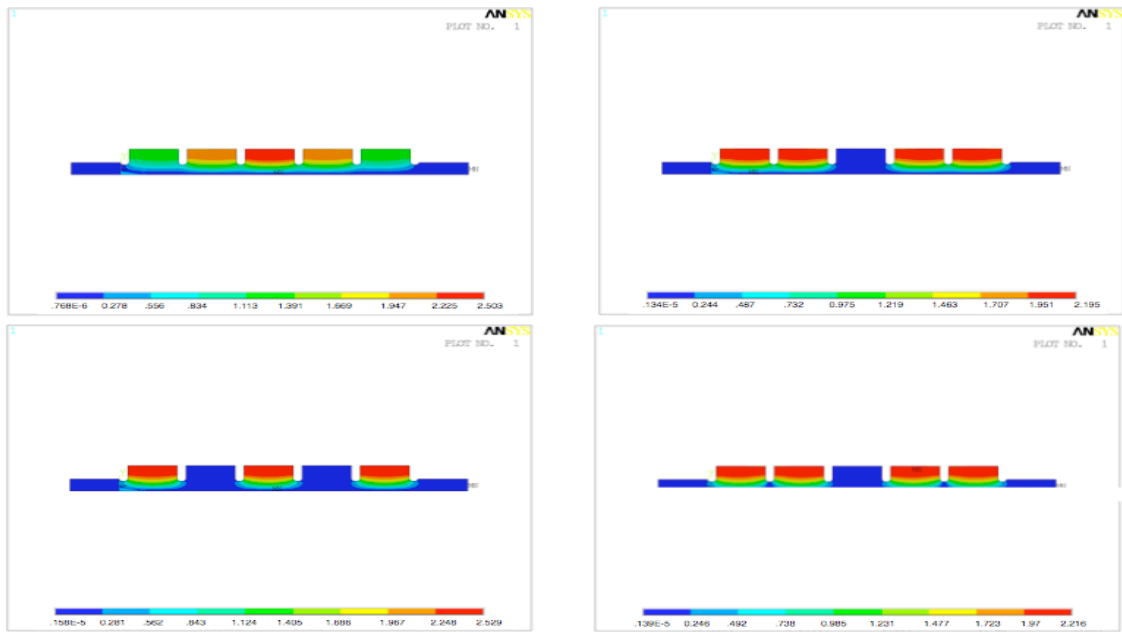


Figure 21: Magnetic Field Intensity (H [A/m]).

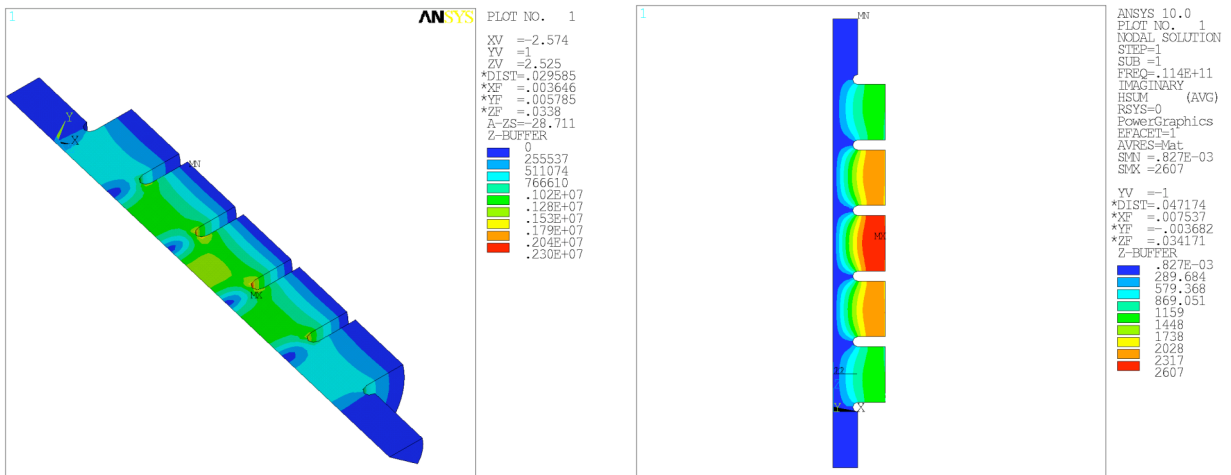


Figure 22: The π -mode (11.4 GHz): on the left: the Electric Field[V/m]; on the right the Magnetic Field Intensity [A/m].

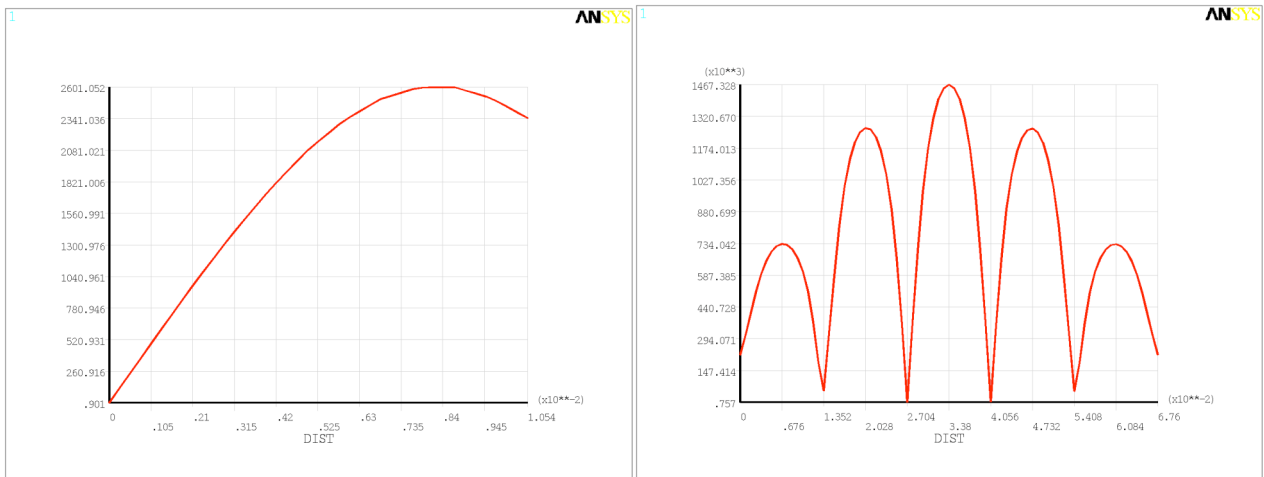


Figure 23: The π -mode (11.4 GHz). On the left: the radial profile of H(A/m) in the middle of the cavity; on the right: the axial profile of the Electric Field (vector sum) [V/m].

3.2.2 Harmonic Analysis

In order to evaluate the power loss induced in the skin depth of the copper surface, an harmonic excitation at 11.4 GHz working frequency has been applied to the cavity. This means that the cavity, in our calculations, is supposed to work in continuous regime at the π -mode⁷. The excitation has been applied by using a suitable modal port, this being a new feature available on the last version of ANSYS (10.0). Using the macro 'HFMODPRT' it is possible to calculate the electromagnetic field distribution for a modal port⁸. This command must be issued in solution phase, having previously defined a modal port by the hfport command. We applied the modal port load on the nodes of a plane surface in the center of one external cell of the cavity.

The excitation of the resonance can be obtained for different values of the peak magnetic field, or in equivalent way, for different values of electromagnetic power stored per cycle in the cavity. We have chosen the first option and by means of interactive calculations (driven by the knowledge of the theoretical field expected, according to the equation 3) we found the electromagnetic field corresponding to 37.5 W of power loss (in fact only a quarter of the whole structure only has been modeled), obtaining the following values, respectively for the electric and magnetic field: $E=1.47 +i(3.8E-6)$ MV/m; $H=6.7 +i(2601)$ A/m. This has been done because essentially we want to compare the simulation results with the experimental values obtained when 150 W are generated in the thermal heater and transferred by radiation.

$$P_{loss} = \frac{R_w}{2\mu_0^2} \int_{S_{cavity}} B^2 dS \quad (3)$$

During our study a possible bug in ANSYS, in the assignment of the surface resistivity has been found. This has been already communicated to the Italian ANSYS assistance that is going to do more accurate check on this problem. In fact, the maximum magnetic field intensity that is expected on the cavity surface in order to have an average power loss of 150 W is of the order of few thousand in A/m for our cavity. According the ANSYS manual, on applying loads in case of High Frequency electromagnetic analysis, the power loss for HF119 elements are calculated assigning the surface resistivity to the nodes of the internal cavity wall, using the <sf,node,shld,Z,1> instruction. The keyword shld allows to specify that we are concerned by a non perfect electric conductor, whose surface conductivity has to be specified by the Z parameter, that should be estimated by the following equation:

$$Z = \sqrt{\frac{\omega\mu_0\mu_r}{2\sigma}} \quad (4)$$

where, as well known,

1. μ_0 is the free-space permeability (1.256 E-6 N/A²).
2. μ_r is the relative permeability.
3. σ is the conductivity of the non-perfect electric conductor (59.6E+6 S/m).

⁷ Calculations to take into account the real duty cycle of the cavity have been planned. Note that ANSYS doesn't allow to perform transient calculations with HF119 elements.

⁸ The command HFMODPRT automatically generates, at the frequency of interest, a port electromagnetic field by solving the 2D eigenvalue problem and stores the solution as a 3D Harmonic Excitation and Matching Condition.

For 11.4 GHz, the value that should be used for Z is 35.9 in mks units, but in this case ANSYS calculates a magnetic field intensity of only few A/m to obtain 37.5 W of surface power loss. On the contrary if we use the standard conductivity σ in place of Z , the code gives the correct expected order of magnitude of the magnetic field H corresponding to the specified power loss.

3.2.3 RF Power Loss Estimation

Among the output data obtainable from the electromagnetic solution (associated with the HF119 element), the following item is essentially used to derive the thermal load (power loss) to be applied on the vacuum-cavity interface nodes:

- HFLXAVG: the heat flux across the element faces caused by surface power losses

We have written a macro that for each element that has, at least, a face in contact with the vacuum-cavity wall, extracts the heat flux value (hflxavg output parameter), corresponding to the heat flow rate across the contact faces of the selected elements. Finally the macro records these values in a table. With another macro we transfer the heat flow rate of each element as surface load on the corresponding nodes belonging to the inner wall of the cavity. Before launching the calculation we checked that the total sum on the inner surface of the hflxavg values in the table coincides exactly the surface loss value, estimated by the macro POWERH. This is a built-in macro that calculates the time-averaged (rms) power loss in a conductor or lossy dielectric material from an harmonic analysis. We can see the distribution of the calculated thermal heat flux in figure 24 (surface load reported in W/m^2).

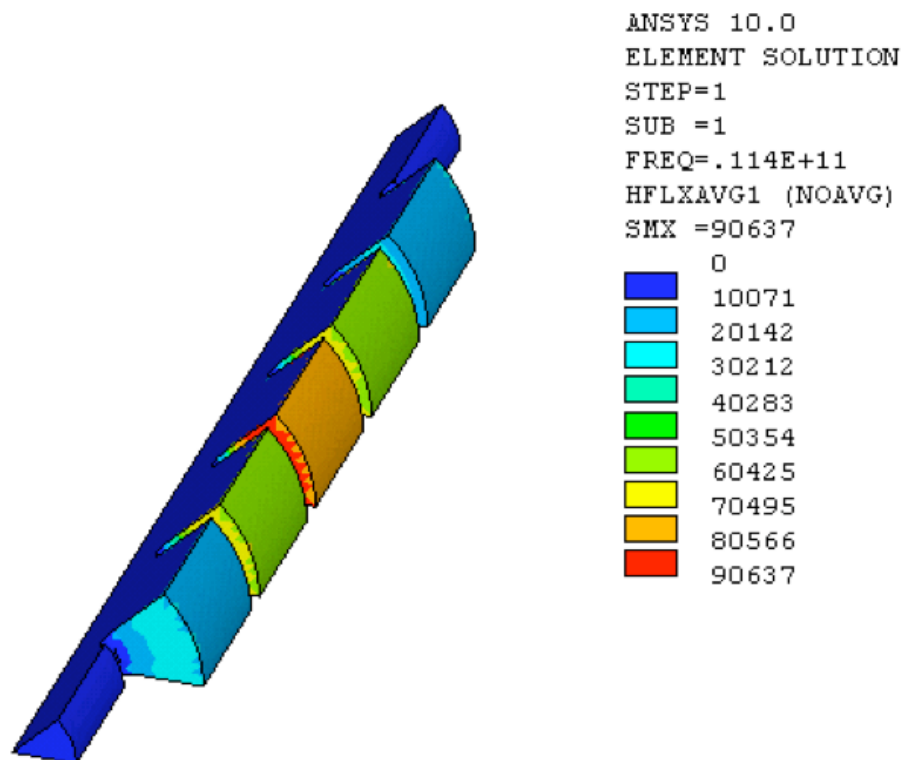


Figure 24: Surface Power Loss [W/m^2].

3.2.4 Thermal Analysis Results

Coupling analysis means that the results of simulations in one domain are used as input for the other domain. In this case we meshed the copper cavity model (for a total number of 65541 elements) and apply loads and boundary condition to it, after having deleted the previous elements corresponding to the vacuum space. The unmeshed model is shown in figure 25, together with the copper cavity mesh.

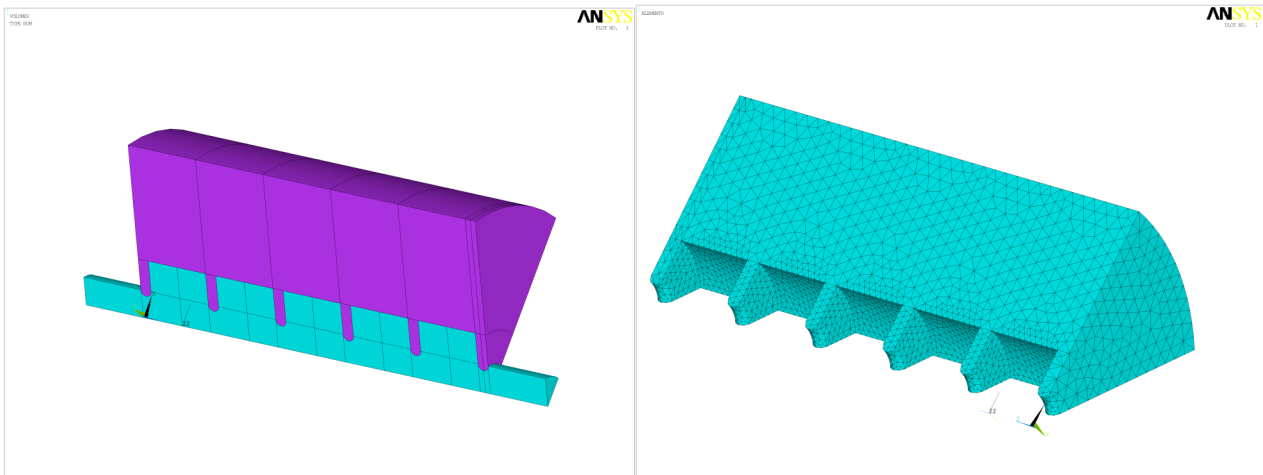


Figure 25: On the left: unmeshed volumes; on the right copper structure's mesh.

We did two calculations, corresponding to the same thermal load input (150 W) but with different boundary conditions: in the first one we have supposed to have the external boundary temperature equal to 298 K and the second one equal to 304 K. Figure 26 shows the temperature profile in the whole cavity for 298 and 304 K external temperature, respectively, while in figure 27, the radial profile of the temperature on the two central irises (up-to the external boundary) is shown.

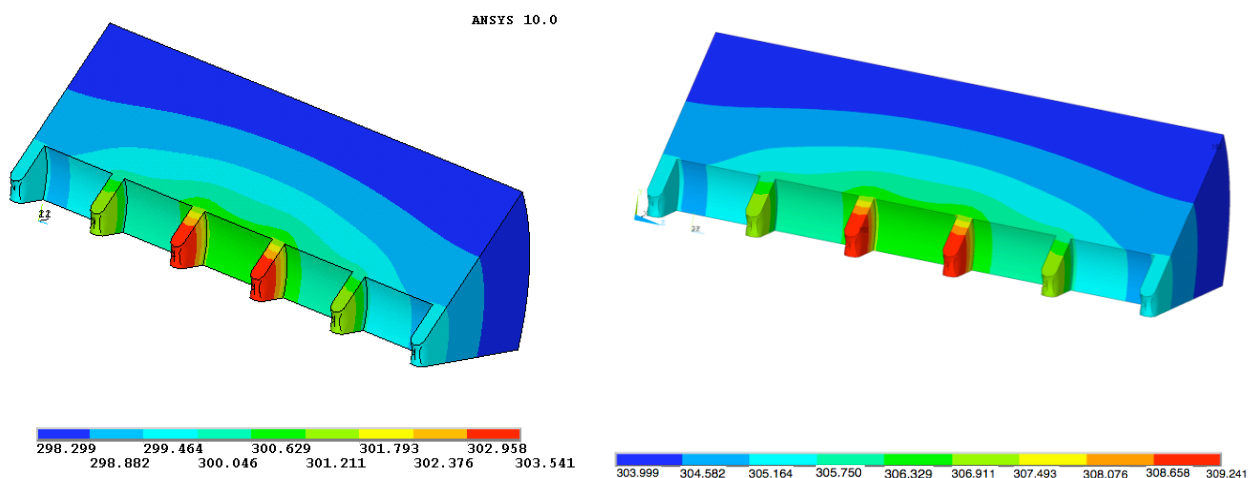


Figure 26: Temperature map in the copper cavity for a thermal load of 150 W and a boundary surface temperature of 298 K on the left and 304 on the right.

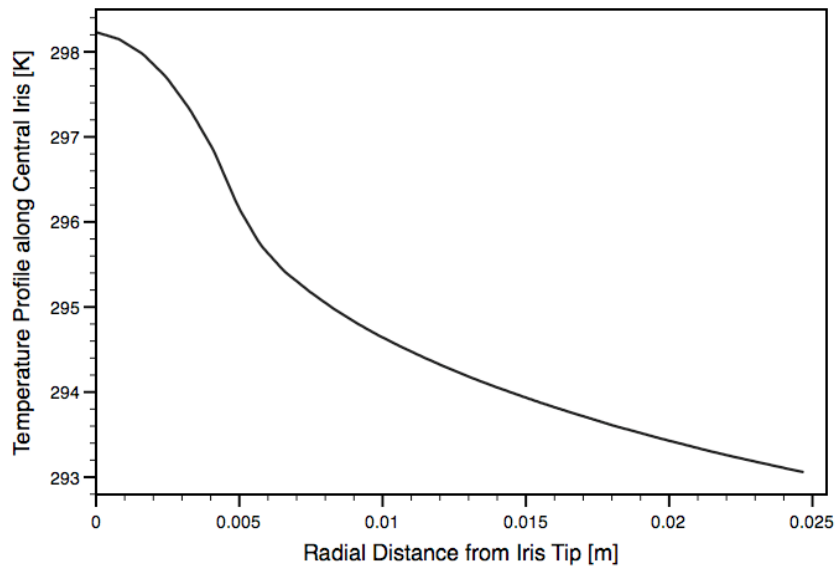


Figure 27: Radial Temperature Profile from the tip of the central irises to the external boundary (150 W surface power loss).

The axial temperature distribution is similar to that induced by the thermal heater, even if in the radiation heating calculation we obtained a flatter profile with isothermal curves almost parallel to the cylindrical inner wall. In case of thermal load from power loss (for a not compensated cavity) the axial temperature profile is more peaked in the middle (see figure 28), with larger temperature gradients in axial direction than that estimated in case of radiation from an internal heater.

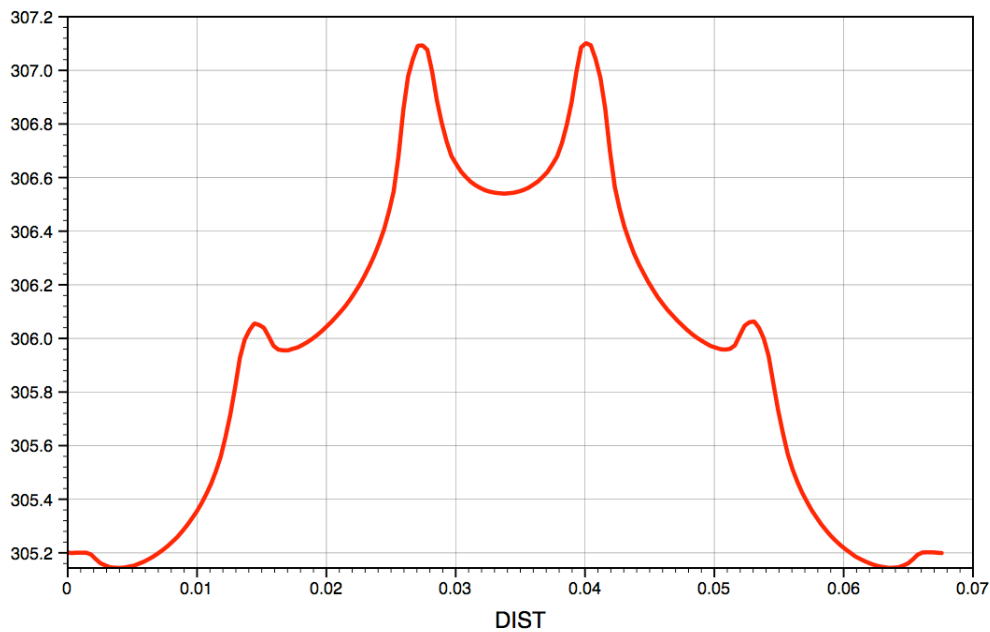


Figure 28: Axial temperature profile in the cavity (150 W of power loss and 304K on the external boundary), along the diameter at the iris bases.

Anyway, we want to stress again that for a well-compensated cavity (for which the difference between the EM-field in the external and internal cells has been reduced to few percent) we expect a longitudinal temperature profile quite similar to that obtained for the radiation thermal heater.

Like in the radiation heater case, the maximum difference of temperature is in the middle of the cavity: $T_{\max}=5\text{K}$, and, as expected, the maximum difference of temperature doesn't depend on the boundary condition. In fact we made a steady-state calculation: the total outgoing flux has to be equal to the input flux because the internal energy cannot change. The total thermal flux is proportional to the average temperature gradient in the volume and because the thermal conductivity is constant, the T_{\max} is fixed by the input power, according the well known Fourier Heat Equation, that in steady state condition becomes:

$$q'' = k \cdot \nabla T \quad (5)$$

where k is the thermal conductivity of the material and q'' is the heat flux per unit surface .

4 Conclusion

An experimental technique, that can be easily and cheaply implemented in the laboratory, has been proposed for preliminary testing the mechanical deformations caused by a temperature gradient profile as close as possible to the real one induced by the electromagnetic power loss. The knowledge of the thermal strains allows evaluating the frequency shifts of the cavity modes in order to assess a tuning strategy.

The aim of this work is to compare, by computer simulations with the ANSYS code, the temperature profile in an X-band linac structure, in the case of radiation heating and in the case of rf-surface power loss (for the same input power), in order to check the similarity of the thermal distributions for the two cases, analyze the difference between them and individuate possible limits of the proposed method.

Experiments have been performed with a radiator and the measured temperature in the cavity is compared with the computed one, for several values of the input heating. The result of this analysis is that the calculated values reproduce the experimental results with an average accuracy better than 20%, that can be sufficient for the validation of the finite-element model used for the radiation heating calculations.

By exploiting the ability of the ANSYS code to link electromagnetic and thermal analyses, we have estimated the temperature profile inside the cavity when it is operating at 11.4 GHz resonance (π -mode). A coupled-field analysis by a single code allows evaluating the RF losses and the consequent temperature distribution in the cavity with better accuracy than that obtained by the exchange of information between different numerical codes.

The analysis of the simulations has confirmed that the axial temperature distribution is similar to that induced by the thermal heater, even if some difference have been found and discussed.

In fact the isotherm curves inside the cavity in the case of radiation heating are flatter than that obtained in the case of surface power loss. Anyway we expect that this difference should become less important when the electro-magnetic field compensation of the multi-cell cavity is taken into account.

Acknowledgements

This work has been made possible thanks to the fundamental support of Bruno Spataro that has proposed the idea of the analyzed experimental technique and thanks to the experimental work of S. Bini, P. Chimenti, V. Chimenti, R. Di Raddo, V. Lollo: we appreciate all of them very much for their helpful cooperation.

References

- [1] S. Bini, P. Chimenti, V. Chimenti, R. Di Raddo, V. Lollo, B. Spataro, F. Tazzioli: Thermal Measurements on a RF 11,4 GHz Accelerating Structure, SPARC-RF-06/003, 29/09/2006 .
- [2] D. Alesini et al.: The SPARC Project: A High Brightness Electron Beam Source at LNF to Drive a SASE-FEL Experiment, presented at PAC2003, 12-16/5/2003, Portland, Oregon, USA.
- [3] ANSYS is a trademark of SAS Inc. www.ansys.com